*31st EPS Conference on Plasma Phys. London, 28 June - 2 July 2004 ECA Vol.**28G**, P-4.198 (2004)*

Simulation of Neoclassical Effects with B2SOLPS5.0 for MAST

V. Rozhansky[1], E. Kaveeva[1], S. Voskoboynikov[1], G. Counsell[2], A. Kirk[2],
D. Coster[3], R. Schneider[4]

[1]*St.Petersburg State Polytechnical University, St.Petersburg, Russia*
[2]*EURATOM/UKAEA Fusion Association, Culham Science Centre, Abingdon, Oxon, UK*
[3]*Max-Planck Institut für Plasmaphysik, EURATOM Association, Garching, Germany*
[4]*Max-Planck Institut für Plasmaphysik, EURATOM Association, Greifswald, Germany*

Introduction

A detailed modeling of the edge plasma of the MAST spherical tokamak was performed with the B2SOLPS5.0 2D transport code [1]. This code is able to reproduce all neoclassical effects [2] since the equations solved are reduced to Pfirsch-Schlueter classical equations, when the anomalous transport coefficients are replaced by their classical values. In the real experiments neoclassical effects on the closed flux surfaces exist in combination with strong anomalous particle, heat and momentum transport in the presence of sources and sinks, and therefore it was unclear to which extent neoclassical results are valid in the separatrix vicinity. Neoclassical effects should be more pronounced in MAST than in the standard tokamaks due to its tight aspect ratio. Below the role of neoclassical mechanisms in the edge plasma on closed flux surfaces is investigated on the basis of numerical simulation. The neoclassical contribution to the particle and heat fluxes is also studied.

Simulations

The Ohmic L-mode Disconnected Double Null MAST discharge №6467 (active lower divertor) was modeled. The anomalous diffusion coefficient $D = 1.5\ m^2/s$, electron and ion heat conductivities $\kappa_e / n_e = 2.5\ m^2/s$, $\kappa_i / n_e = 3.75\ m^2/s$ were chosen. The plasma density at the inner boundary (6 *cm* inside the separatrix at the outer midplane) was $n_e|_{core} = 1.75 \cdot 10^{19} m^{-3}$ according to the experimental density profile, the electron and ion temperatures are $T_e|_{core} = 120\,eV$, $T_i|_{core} = 120\,eV$. Gas puff of $\Gamma = 6.3 \cdot 10^{21}\ s^{-1}$ was imposed at the outer midplane (poloidally distributed over the distance ~1 *m*). The simulation for the shot №6468 with inboard gas puff $\Gamma = 6.3 \cdot 10^{21}\ s^{-1}$ and similar geometry and plasma parameters was also performed. The experimentally observed electron temperature and density radial profiles at the outer and inner midplanes as well

as the saturation current and electron temperature distributions at the divertor plates are reproduced in the simulations (with accuracy of the order of two near the plates).

It is known from neoclassical theory [2] that the parallel ion heat flux, which closes the vertical heat flux caused by ion ∇B drift, is directed from the lower to the upper part of the torus (∇B drift of ions is directed towards lower X-point)

$$q_{\parallel}^{P.S.} = \frac{5}{2}\frac{n_e T_i}{e}\frac{\partial T_i}{h_y \partial y}\frac{B_z}{B_x B}\left(1 - \frac{B^2}{\langle B^2 \rangle}\right) \qquad (1)$$

Here x and y are poloidal (directed from the inner to the outer plate) and radial coordinates respectively, h_x, h_y are metric coefficients. For shot №6467 the parallel ion heat flux calculated in the code was close to Eq. (1), Fig. 1. To provide this flux the ion temperature perturbation on the flux surface has to be formed, Fig. 2. The poloidal ion temperature perturbation is very pronounced (of the order of 20%), in accordance with neoclassical predictions and has a maximum at the lower part of the torus. In the estimate of the ion temperature perturbation it should be taken into account that plasma in MAST inside the separatrix is in the plateau regime. The density poloidal perturbation may be calculated from the condition of constant total pressure on the flux surface: $p = n_e(T_e + T_i) = const$ (since the parallel velocity is much smaller than the sound speed) and constant T_e. It is very close to that obtained in the simulations, Fig. 3. The perturbation of electrostatic potential, which corresponds to the Boltzmann distribution of electrons $\delta\varphi = (T_e / e)\ln n_e$ +const, is also close to simulations, Fig.4.

The particle flux consists of anomalous flux and a small neoclassical correction, Fig.5. The neoclassical particle flux may be considered as a sum of two contributions, one from the $\vec{E} \times \vec{B}$ flux ($\oint n_e V_y^{E\times B} ds$) and another one from the ∇B drift flux ($\oint n_e \tilde{V}_y^{(dia)} ds$). In agreement with the prediction of neoclassical theory these two fluxes almost completely compensate each other after integration over the flux surface. The situation for the electron heat flux is quite similar, Fig.6. At the same time, the neoclassical contribution to the ion heat flux in MAST is significant, Fig.7. The neoclassical ion heat conductivity is larger than the neoclassical electron heat conductivity by a factor $k_i^{NEO} / k_e^{NEO} = (m_i / m_e)^{1/2}$, while the anomalous heat conductivities are of the same order. Note that in the standard tokamak geometry in L-mode the contribution from both the ion and electron neoclassical heat fluxes is negligible, see simulations for ASDEX Upgrade

[3]. In contrast, in MAST the ion neoclassical heat flux is of the order of the anomalous heat flux even for L-regime.

In the case of inboard gas puffing, shot №6468, the temperature, density and potential perturbations are shifted considerably poloidally towards the HFS due to the heat sink associated with neutrals, Fig. 8. In spite of this fact the drift (neoclassical) contribution to ion heat flux does not change considerably, Fig. 9.

The calculated radial electric field profile for shot №6467 at the outer mid-plane is shown in Fig. 10. In the core region the radial electric field is close to the neoclassical electric field, both for outboard gas puffing shot №6467 and inboard gas puffing shot №6468. This electric field is similar to that simulated for standard tokamaks [1].

Conclusions

According to the simulations in MAST spherical tokamak the neoclassical effects exist in spite of the presence of strong anomalous fluxes. The neoclassical ion heat flux is comparable with the anomalous radial ion heat flux and neutral heat flux in L-regime, while neoclassical contributions to the particle and electron heat fluxes are negligible. The poloidal perturbations of plasma parameters are close to those predicted by neoclassical theory for outboard gas puffing and differ significantly for inboard gas puffing. The radial electric field in the vicinity of the separatrix is close to the neoclassical value.

References

1. V. Rozhansky et al Nucl. Fus. 1110, **41** (2001) 387; V. Rozhansky et al Nucl. Fus. **42** (2002)
2. Hirshman S.P., Sigmar D.J., Nucl. Fusion **21** (1981) 1079
3. V. Rozhansky et al Contrib. Plasma Phys. **44** (2004) 200

Acknowledgements This work was funded jointly by the United Kingdom Engineering and Physical Sciences Research Council and by EURATOM.

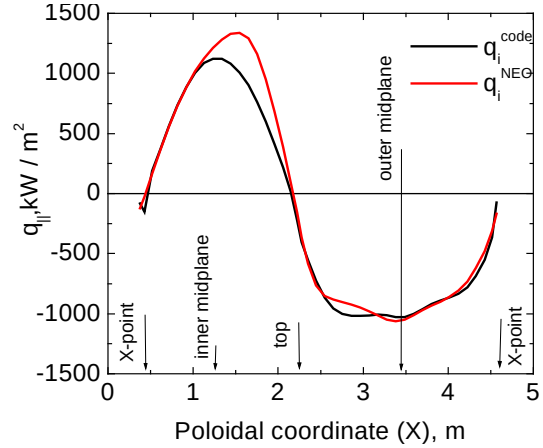

Fig. 1. Parallel heat flux at the closed flux surface 15*mm* inside the separatrix (distance at the outer midplane), shot №6467.

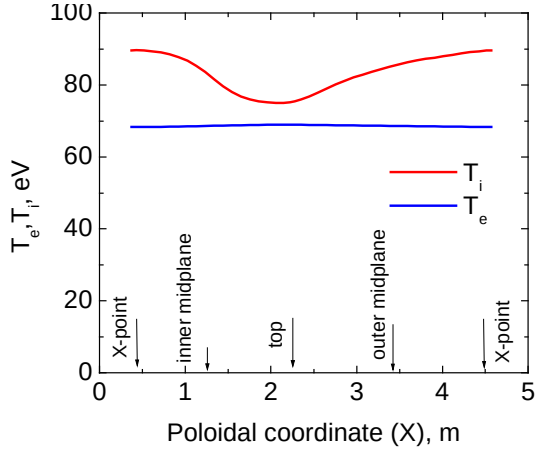

Fig. 2. Poloidal temperature profiles at the closed flux surface 15*mm* inside the separatrix (distance at the outer midplane), shot №6467.

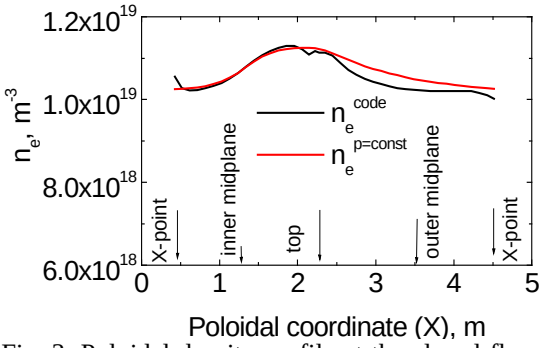

Fig. 3. Poloidal density profile at the closed flux surface 15*mm* inside the separatrix (distance at the outer midplane), shot №6467.

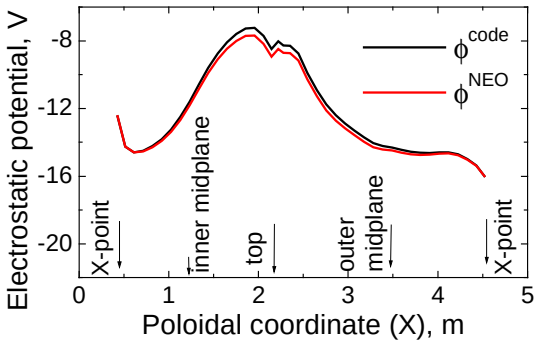

Fig. 4. Poloidal profile of plasma potential at the closed flux surface, shot №6467.

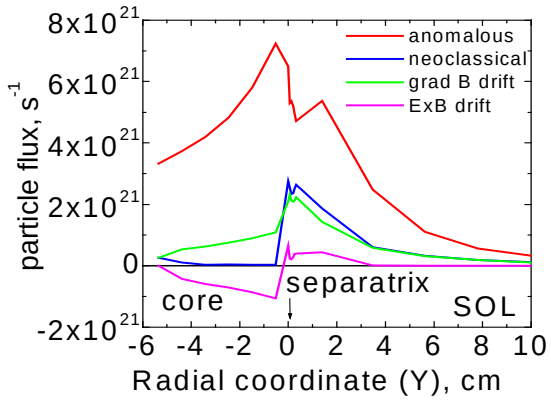

Fig.5. Components of integral particle flux through the flux surface, shot №6467.

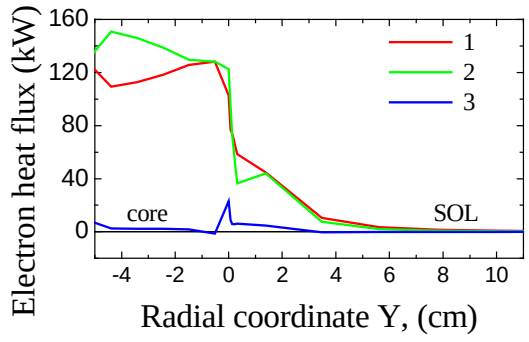

Fig.6. Components of integral electron heat flux through the flux surface, shot №6467.
1- heat flux connected with anomalous diffusion;
2- anomalous heat conduction contribution;
3-neoclassical heat flux.

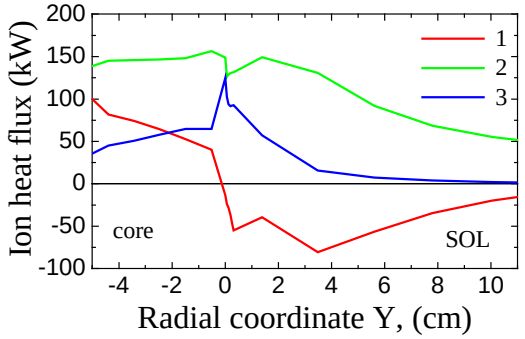

Fig. 7. Components of integral ion heat flux through the flux surface, shot №6467.
1-heat flux caused by anomalous diffusion and convective flux of neutrals;
2-contribution of ion anomalous heat conduction and neutral heat conduction;
3-neoclassical heat flux.

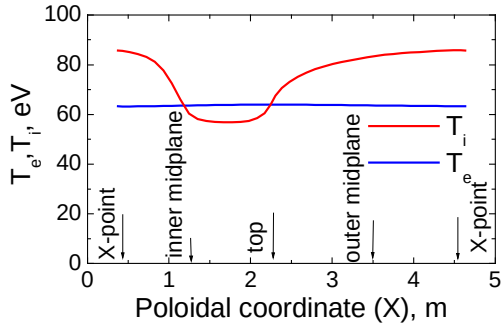

Fig. 8. Poloidal temperature profiles at the closed flux surface **for inboard puffing,** shot №6468.

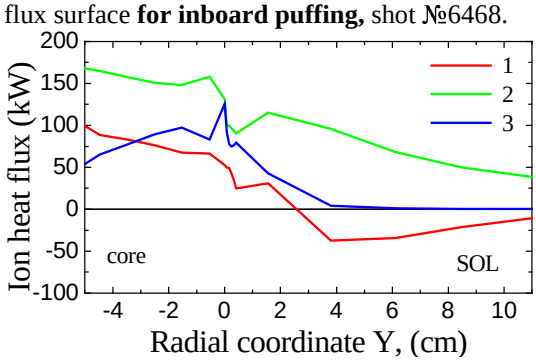

Fig. 9. Components of integral ion heat flux through the flux surface **for inboard puffing,** shot №6468. Notations are the same as in Fig.7.

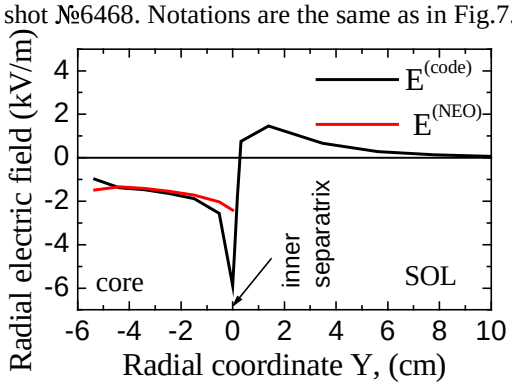

Fig. 10. Radial electric field at the outer midplane for MAST shot №6467.